

Simulation of Multicomponent Aerosol Dynamics

FRED GELBARD¹

Environmental Research, 4533, Sandia Laboratories, Albuquerque, New Mexico 87185

AND

JOHN H. SEINFELD

Department of Chemical Engineering, California Institute of Technology, Pasadena, California 91125

Received February 11, 1980; accepted May 12, 1980

A general technique for simulating the evolution of aerosol size and chemical composition distributions resulting from (1) coagulation, (2) intraparticle chemical reaction, (3) gas-to-particle conversion, and (4) particle sources and removal mechanisms is developed. The technique is based upon dividing the particle size domain into m arbitrarily located sections and imposing the condition of mass conservation for each component. The technique, which is shown to be computationally attractive when compared with other potential approaches, is illustrated through simulating the influence of a source of small particles on the evolution of a mixed plume and background aerosol consisting of three chemical species.

I. INTRODUCTION

In the study of atmospheric aerosols, much effort has been devoted to understanding the physical and chemical mechanisms of aerosol evolution. For a spatially homogeneous aerosol, particles are characterized by size and chemical composition. Nearly all previous work on solving the governing equations for spatially homogeneous aerosols focused on the evolution of the particle size distribution as affected by coagulation (1–5), condensational growth (6–8), and sources and removal mechanisms (9–12). Although one often must deal with aerosols that consist of several species, a notable example being atmospheric aerosols, little work has been reported on solving the governing equations for the evolution of the multicomponent chemical composition distribution function. To obtain

analytical solutions of the governing equation for a multicomponent aerosol, previous works (13, 14) resorted to simplified cases which are of limited value for describing actual aerosols. Since particle chemical composition is very important in determining human health effects, studies restricted to size distribution dynamics cannot fully assess aerosol health effects. Furthermore, the chemical composition of a particle often affects its growth rate, and thus the computation of the size distribution often may not be performed independently of that for the composition dynamics of the aerosol.

In this work a general method for simulating the evolution of the distribution of chemical species with respect to aerosol particle size is developed. The physical phenomena included are: (i) coagulation, (ii) intraparticle chemical reaction, (iii) gas-to-particle conversion, and (iv) particle sources and removal mechanisms. Thus, for the first time a technique is presented that

¹ Present address: Department of Chemical Engineering, Massachusetts Institute of Technology, Cambridge, Mass. 02139.

computes not only the evolving size distribution but also the variation of chemical composition with particle size.

The technique (as discussed for one-component systems in (15)) is based upon dividing the particle size domain into m arbitrarily located sections and imposing the condition of mass conservation for each component for the four processes given above. In Part II, a detailed derivation of the conservation equations is presented. It is shown that for a system of s components, a set of $m \times s$ ordinary differential equations results. To demonstrate the novel capabilities of the resulting multicomponent sectional equations, we simulate the influence of a source of small particles on the evolution of an aerosol which may have formed from the mixing of a power plant plume with a background aerosol. In Part III, the simulation results are discussed and it is shown that by using the multicomponent equations presented in this work, the processes that result in the formation and movement of aerosol mass to larger particle sizes can be displayed, and hence better understood, in a manner not previously possible with the conventional one-component equations. Finally, in Parts IV and V, we conclude with a discussion of the computing requirements of the new technique as compared to other possible alternatives for simulating multicomponent aerosol dynamics.

II. GOVERNING EQUATIONS FOR A MULTICOMPONENT SECTIONAL REPRESENTATION

We consider a spatially homogeneous aerosol in which particle size is characterized by a single variable v , typically particle mass, which is conserved during coagulation and intraparticle chemical reactions. The size distribution function $n(v, t)$ is defined such that $n(v, t)dv$ is the number concentration of particles in the range $[v, v + dv]$ at time t . By dividing the entire particle size domain into m contiguous arbi-

trarily sized sections and defining Q_l as the total mass of aerosol per unit volume of fluid in section l at time t we have

$$Q_l(t) = \sum_{k=1}^s Q_{l,k}(t) = \int_{v_{l-1}}^{v_l} vn(v, t)dv, \quad [1]$$

where $Q_{l,k}(t)$ is the mass of component k in section l , s is the total number of components, and v_{l-1} and v_l denote the size of the smallest and largest particles, respectively, in section l . Note that v_0 is arbitrary and the upper bound of section $l - 1$ is equal to the lower bound of section l for $l = 2, 3, \dots, m$.

In our previous work on sectional equations (15), the general conservation equations were derived such that any integral property of the aerosol size distribution (e.g., number, surface area, or volume) was conserved. Since this work is concerned with multicomponent aerosols, the concept of a number or surface area concentration of a single component in a particle composed of a mixture of s components has little physical significance and thus only conservation of mass is considered. Therefore, our objective in this work is to derive the general conservation equations for $Q_{l,k}$ ($l = 1, 2, \dots, m$ and $k = 1, 2, \dots, s$).

The conservation equations are derived by determining the net rates at which species k is added to each section by (i) coagulation, (ii) intraparticle chemical reaction, (iii) gas-to-particle conversion, and (iv) particle sources and removal mechanisms. The expressions for each of the above mechanisms will be derived in Parts II.A–II.D, respectively. In Part II.E, the final set of sectional equations will be obtained by combining the terms in Parts II.A–II.D.

A. Coagulation

We assume only binary collisions occur and that the rate of coagulation between particles in the mass ranges $[u, u + du]$ and $[v, v + dv]$ is given by $\beta(u, v)n(u, t)n(v, t) \times dudv$, where $\beta(u, v) = \beta(v, u)$ is the co-

agulation coefficient which is dependent only on the total masses of the coagulating particles. For particles in sections lower than l , the total rate of coagulation is given by

$$\frac{1}{2} \int_{v_0}^{v_{l-1}} \int_{v_0}^{v_{l-1}} \beta(u, v) n(u, t) n(v, t) du dv. \quad [2]$$

However, only if the resulting particle is in the range $[v_{l-1}, v_l]$ is it added to section l . Therefore, we introduce the function θ , which is equal to one if the specified condition is satisfied and zero if it is not. Hence,

$$\theta(v_{l-1} < u + v < v_l) = \begin{cases} 1 & v_{l-1} < u + v < v_l \\ 0 & \text{otherwise.} \end{cases} \quad [3]$$

Using [3], the flux of mass into section l by coagulation of particles in lower sections may be expressed as

$$\frac{1}{2} \int_{v_0}^{v_{l-1}} \int_{v_0}^{v_{l-1}} \theta(v_{l-1} < u + v < v_l) (u + v) \times \beta(u, v) n(u, t) n(v, t) du dv. \quad [4]$$

Notice that the factor $(u + v)$ was incorporated into the integrand of [4] to determine the mass entering section l . Since the mass of each component is conserved by coagulation, the flux of mass of component k into section l is given by the sum of the masses of component k in the coagulating particles. In general, particles of the same size may have different compositions and thus composition may not be a unique function of particle size. Therefore, one can define a marginal mass fraction probability density function $g_k(v, \eta_k)$, where $0 \leq \eta_k \leq 1$, and $g_k(v, \eta_k) d\eta_k$ is the time-dependent fraction of particles in the mass range $[v, v + dv]$ with a mass fraction of component k in the range $[\eta_k, \eta_k + d\eta_k]$. Thus, for $k = 1, 2, \dots, s$,

$$\int_0^1 g_k(v, \eta_k) d\eta_k = 1 \quad [5]$$

and $g_k(v, \eta_k) n(v, t) dv d\eta_k$ is the number concentration of particles in the size range $[v, v + dv]$ with a mass fraction of component k in the range $[\eta_k, \eta_k + d\eta_k]$. Since the mass concentration of component k for a particle in the size range $[v, v + dv]$ is given by

$$\left\{ \int_0^1 v \eta_k g_k(v, \eta_k) d\eta_k \right\} n(v, t) dv, \quad [6]$$

the mass flux of component k into section l is

$$\frac{1}{2} \int_{v_0}^{v_{l-1}} \int_{v_0}^{v_{l-1}} \theta(v_{l-1} < u + v < v_l) \times \int_0^1 \int_0^1 (u \xi_k + v \eta_k) g_k(u, \xi_k) g_k(v, \eta_k) \times d\xi_k d\eta_k \beta(u, v) n(u, t) n(v, t) du dv. \quad [7]$$

Using the property of $g_k(v, \eta_k)$ given in Eq. [5], [7] reduces to

$$\frac{1}{2} \int_{v_0}^{v_{l-1}} \int_{v_0}^{v_{l-1}} \theta(v_{l-1} < u + v < v_l) \times \left\{ u \int_0^1 \xi_k g_k(u, \xi_k) d\xi_k + v \int_0^1 \eta_k g_k(v, \eta_k) d\eta_k \right\} \times \beta(u, v) n(u, t) n(v, t) du dv. \quad [8]$$

By defining the mean mass of component k for all particles having mass in the range $[v, v + dv]$ as

$$\begin{aligned} \bar{v}_k &= \int_0^1 v \eta_k g_k(v, \eta_k) d\eta_k \\ &= v \int_0^1 \eta_k g_k(v, \eta_k) d\eta_k, \end{aligned} \quad [9]$$

[8] can be reduced to

$$\frac{1}{2} \int_{v_0}^{v_{l-1}} \int_{v_0}^{v_{l-1}} \theta(v_{l-1} < u + v < v_l) (\bar{u}_k + \bar{v}_k) \times \beta(u, v) n(u, t) n(v, t) du dv, \quad [10]$$

where

$$\begin{aligned}\bar{u}_k &= \int_0^1 u \xi_k g_k(u, \xi_k) d\xi_k \\ &= u \int_0^1 \xi_k g_k(u, \xi_k) d\xi_k.\end{aligned}\quad [11]$$

Notice that [10] is similar to [4] except that one uses the mean mass of a component instead of the total mass of the particle to determine the mass flux of a specific component into section l .

Particles and hence mass are removed from section l when a particle from section l coagulates with a particle from a lower section and forms a particle larger than v_l . The rate at which such events occur is given by

$$\begin{aligned}\int_{v_0}^{v_{l-1}} \int_{v_{l-1}}^{v_l} \theta(u + v > v_l) \\ \times \beta(u, v) n(u, t) n(v, t) dudv.\end{aligned}\quad [12]$$

Therefore, the flux of component k out of section l is given by

$$\begin{aligned}\int_{v_0}^{v_{l-1}} \int_{v_{l-1}}^{v_l} \theta(u + v > v_l) \bar{u}_k \\ \times \beta(u, v) n(u, t) n(v, t) dudv.\end{aligned}\quad [13]$$

However, if a particle in a section lower than l coagulates with a particle in section l and the resulting particle remains in section

l , the flux of component k into section l is given by

$$\begin{aligned}\int_{v_0}^{v_{l-1}} \int_{v_{l-1}}^{v_l} \theta(u + v < v_l) \bar{v}_k \\ \times \beta(u, v) n(u, t) n(v, t) dudv.\end{aligned}\quad [14]$$

Intrasectional coagulation can only remove mass if the resulting particle size is greater than v_l for the l th section. Therefore, the mass flux of component k out of section l by intrasectional coagulation is given by

$$\begin{aligned}\frac{1}{2} \int_{v_{l-1}}^{v_l} \int_{v_{l-1}}^{v_l} \theta(u + v > v_l) (\bar{u}_k + \bar{v}_k) \\ \times \beta(u, v) n(u, t) n(v, t) dudv.\end{aligned}\quad [15]$$

Finally, for $l < m$ the mass flux of component k leaving section l by coagulation of particles within section l and those of higher sections is given by

$$\int_{v_l}^{v_m} \int_{v_{l-1}}^{v_l} \bar{u}_k \beta(u, v) n(u, t) n(v, t) dudv.\quad [16]$$

Notice that in [16] the θ function is not required since all coagulations of particles in section l with particles in higher sections will remove a particle from section l .

Combining the terms in [10], [13]–[16] the sectional equations for $Q_{l,k}$ ($l = 1, 2, \dots, m$ and $k = 1, 2, \dots, s$) for an aerosol undergoing only coagulation are

$$\begin{aligned}\frac{dQ_{l,k}}{dt} &= \frac{1}{2} \int_{v_0}^{v_{l-1}} \int_{v_0}^{v_{l-1}} \theta(v_{l-1} < u + v < v_l) (\bar{u}_k + \bar{v}_k) \beta(u, v) n(u, t) n(v, t) dudv \\ &\quad - \int_{v_0}^{v_{l-1}} \int_{v_{l-1}}^{v_l} \theta(u + v > v_l) \bar{u}_k \beta(u, v) n(u, t) n(v, t) dudv \\ &\quad + \int_{v_0}^{v_{l-1}} \int_{v_{l-1}}^{v_l} \theta(u + v < v_l) \bar{v}_k \beta(u, v) n(u, t) n(v, t) dudv \\ &\quad - \frac{1}{2} \int_{v_{l-1}}^{v_l} \int_{v_{l-1}}^{v_l} \theta(u + v > v_l) (\bar{u}_k + \bar{v}_k) \beta(u, v) n(u, t) n(v, t) dudv \\ &\quad - \int_{v_l}^{v_m} \int_{v_{l-1}}^{v_l} \bar{u}_k \beta(u, v) n(u, t) n(v, t) dudv.\end{aligned}\quad [17]$$

To obtain the contribution of the various sections to $Q_{l,k}$, one replaces the integrals

in Eq. [17] that range over more than one section by a sum of integrals over each section.

$$\begin{aligned} \frac{dQ_{l,k}}{dt} = & \frac{1}{2} \sum_{i=1}^{l-1} \sum_{j=1}^{l-1} \int_{v_{i-1}}^{v_i} \int_{v_{j-1}}^{v_j} \theta(v_{l-1} < u + v < v_l) (\bar{u}_k + \bar{v}_k) \beta(u, v) n(u, t) n(v, t) du dv \\ & - \sum_{i=1}^{l-1} \int_{v_{i-1}}^{v_i} \int_{v_{l-1}}^{v_l} \theta(u + v > v_l) \bar{u}_k \beta(u, v) n(u, t) n(v, t) du dv \\ & + \sum_{i=1}^{l-1} \int_{v_{i-1}}^{v_i} \int_{v_{l-1}}^{v_l} \theta(u + v < v_l) \bar{v}_k \beta(u, v) n(u, t) n(v, t) du dv \\ & - \frac{1}{2} \int_{v_{l-1}}^{v_l} \int_{v_{l-1}}^{v_l} \theta(u + v > v_l) (\bar{u}_k + \bar{v}_k) \beta(u, v) n(u, t) n(v, t) du dv \\ & - \sum_{i=l+1}^m \int_{v_{i-1}}^{v_i} \int_{v_{l-1}}^{v_l} \bar{u}_k \beta(u, v) n(u, t) n(v, t) du dv. \quad [18] \end{aligned}$$

B. Intraparticle Chemical Reaction

Since mass is conserved by intraparticle chemical reaction, no mass can leave or enter a section by this mechanism. However, the mass of individual components can be changed subject to the constraint given in Eq. [1]. In general, the kinetic expressions for the rates of formation and depletion of a component are functions of the concentration of the reactants, and hence functions of particle composition. If $F_k(\eta_1 v, \eta_2 v, \dots, \eta_s v)$ represents the net mass formation rate of component k for a particle of size v with a mass fraction of component i equal to η_i , then

$$\int_{v_{l-1}}^{v_l} F_k(\eta_1 v, \eta_2 v, \dots, \eta_s v) n(v, t) dv \quad [19]$$

is the total mass formation rate of component k in section l per unit volume of fluid. However, since particles of size v may have different compositions, the mass formation rate is given by

$$\int_{v_{l-1}}^{v_l} \left\{ \int_0^1 \cdots \int_0^1 F_k(\eta_1 v, \dots, \eta_s v) \times P d\eta_1 \cdots d\eta_{s-1} \right\} n(v, t) dv, \quad [20]$$

where $P(\eta_1, \dots, \eta_{s-1}, v, t)$ is the joint mass fraction probability density function defined such that

$$P d\eta_1 d\eta_2 \cdots d\eta_{s-1} \quad [21]$$

is the fraction of particles in the size range $[v, v + dv]$ having mass fractions in the ranges $[\eta_1, \eta_1 + d\eta_1], \dots, [\eta_{s-1}, \eta_{s-1} + d\eta_{s-1}]$, and $P = 0$ for $\eta_1 + \eta_2 + \cdots + \eta_{s-1} > 1$. Note that since the sum of η_i ($i = 1, \dots, s$) must be equal to 1, only $s - 1$ mass fractions are independent and therefore only $s - 1$ integrations over particle composition are required in [20]. If F_k is a linear function of its arguments, then

$$F_k = \alpha_{0,k} + \alpha_{1,k} \eta_1 v + \alpha_{2,k} \eta_2 v + \cdots + \alpha_{s,k} \eta_s v, \quad [22]$$

where $\alpha_{i,k}$ ($i = 0, 1, \dots, s$) are arbitrary functions of v and t . Since the expected value of a sum is equal to the sum of the expected values, using Eqs. [5] and [22], [20] can be reduced to

$$\int_{v_{l-1}}^{v_l} (\alpha_{0,k} + \alpha_{1,k} \bar{v}_1 + \alpha_{2,k} \bar{v}_2 + \cdots + \alpha_{s,k} \bar{v}_s) n(v, t) dv \quad [23]$$

for the special case of first-order reactions.

C. Particle Growth by Gas-to-Particle Conversion

Heterogeneous processes which incorporate gaseous species into the particulate phase can alter the size and chemical composition of a particle. In general, gaseous species diffuse to the particle surface and either condense or dissolve in the particle. An analysis for particle growth by these mechanisms followed by chemical reaction on the surface or within the particle has been given elsewhere (8). Since intra-particle reactions are accounted for by the function F_k as discussed in Part II.B, only condensation and dissolution of gaseous species are discussed here.

If the rate at which gaseous molecules of component k of mass v'_k are incorporated into a particle of mass v can be given by $G_k(\eta_1 v, \eta_2 v, \dots, \eta_s v)$, then the mass formation rate of component k in section l is given by

$$\int_{v_{l-1}}^{v_l - v'_k} v'_k G_k(\eta_1 v, \dots, \eta_s v) n(v, t) dv. \quad [24]$$

Notice that the upper limit of integration of [24] is such that particles do not grow larger than v_l since it is assumed that v'_k is small enough such that $v_l - v'_k \geq v_{l-1}$ for $l = 1, 2, \dots, m$ and $k = 1, 2, \dots, s$. When molecules of component i ($i = 1, \dots, s$) of size v'_i are incorporated into particles in the range $[v_l - v'_i, v_l]$, the resulting particle will grow into section $l + 1$. Assuming that molecular additions to a particle occur in series, two different molecular species cannot simultaneously grow a particle out of section l . Therefore, the flux of component k out of section l is given by the sum of the rates at which molecular species grow particles into section $l + 1$. This rate is given by

$$\sum_{i=1}^s \int_{v_{l-1}}^{v_l} v \eta_k G_i(\eta_1 v, \dots, \eta_s v) n(v, t) dv, \quad [25]$$

where $G_i = 0$ if component i is not undergoing gas-to-particle conversion. The flux

of component k into section $l + 1$ is given by

$$\sum_{i=1}^s \int_{v_{l-1}}^{v_l} (v \eta_k + \delta_{i,k} v'_i) G_i(\eta_1 v, \dots, \eta_s v) \times n(v, t) dv, \quad [26]$$

where

$$\delta_{i,k} = \begin{cases} 0 & i \neq k \\ 1 & i = k. \end{cases} \quad [27]$$

For gas-phase diffusion-limited growth, G_k is usually assumed to be proportional to the partial pressure difference of the condensing species in the gas phase and above the particle surface. Since the partial pressure above the particle is generally a function of composition, expressions [24], [25], and [26] must be modified to account for particles of the same size but with different compositions. Thus, the mass formation rate of component k in section l is

$$\int_{v_{l-1}}^{v_l - v'_k} v'_k \left\{ \int_0^1 \dots \int_0^1 G_k(\eta_1 v, \dots, \eta_s v) \times P d\eta_1 \dots d\eta_{s-1} \right\} n(v, t) dv \quad [28]$$

and the flux of component k out of section l is given by

$$\sum_{i=1}^s \int_{v_{l-1}}^{v_l} v \left\{ \int_0^1 \dots \int_0^1 \eta_k G_i(\eta_1 v, \dots, \eta_s v) \times P d\eta_1 \dots d\eta_{s-1} \right\} n(v, t) dv. \quad [29]$$

Finally, the mass flux of component k into section $l + 1$ from section $l < m$ is

$$\sum_{i=1}^s \int_{v_{l-1}}^{v_l} \left\{ \int_0^1 \dots \int_0^1 (\eta_k v + \delta_{i,k} v'_i) \times G_i(\eta_1 v, \dots, \eta_s v) \times P d\eta_1 \dots d\eta_{s-1} \right\} n(v, t) dv. \quad [30]$$

If G_k ($k = 1, \dots, s$) is a linear function of its arguments, then G_k can be expressed as

$$G_k = \gamma_{0,k} + \gamma_{1,k} \eta_1 v + \gamma_{2,k} \eta_2 v + \dots + \gamma_{s,k} \eta_s v, \quad [31]$$

where $\gamma_{i,k}$ ($i = 0, 1, \dots, s$) are arbitrary functions of v and t . For the special case of G_k given by Eq. [31], [28] reduces to

$$\int_{v_{l-1}}^{v_l - v'_k} v'_k (\gamma_{0,k} + \gamma_{1,k} \bar{v}_1 + \gamma_{2,k} \bar{v}_2 + \dots + \gamma_{s,k} \bar{v}_s) n(v, t) dv. \quad [32]$$

If the expected value of the product of the mass fraction of component k in a particle of mass v and the rate at which gaseous molecules of mass v'_i are incorporated into that particle is approximated by the product of the expected value of η_k and the expected value of G_i , the terms in [29] and [30] for G_i given by Eq. [31] reduce to

$$\sum_{i=1}^s \int_{v_l - v'_i}^{v_l} \bar{v}_k (\gamma_{0,i} + \gamma_{1,i} \bar{v}_1 + \gamma_{2,i} \bar{v}_2 + \dots + \gamma_{s,i} \bar{v}_s) n(v, t) dv, \quad [33]$$

$$\sum_{i=1}^s \int_{v_l - v'_i}^{v_l} (\bar{v}_k + \delta_{i,k} v'_i) (\gamma_{0,i} + \gamma_{1,i} \bar{v}_1 + \gamma_{2,i} \bar{v}_2 + \dots + \gamma_{s,i} \bar{v}_s) n(v, t) dv, \quad [34]$$

respectively.

In general, the expected value of a product is not equal to the product of the expected values. However, if the partial pressure of the diffusing gaseous species above the particle surface is negligible compared to that in the gas phase, G_i may be independent of particle composition, in which case the expected values can be factored.

D. Source and Removal Mechanisms

One usually assumes that spatially homogeneous sources are a function of particle

size and time. If $S(v, t)$ represents the source rate such that $S(v, t) dv$ is the generation rate of particles per unit volume of fluid in the size range $[v, v + dv]$ at time t , then

$$\int_{v_{l-1}}^{v_l} v S(v, t) dv \quad [35]$$

is the mass generation rate into section l . Therefore, the generation rate of component k in section l is given by

$$\int_{v_{l-1}}^{v_l} \bar{v}_k S(v, t) dv. \quad [36]$$

To account for a source generating particles of the same size but with different compositions, we use \bar{v}_k to represent the mean mass of component k for generated particles of size v .

In general, removal mechanisms are functions of $n(v, t)$, v , and t . Therefore, if $R[n(v, t), v, t] dv$ is the removal rate of particles in the size range $[v, v + dv]$,

$$\int_{v_{l-1}}^{v_l} \bar{v}_k R[n(v, t), v, t] dv \quad [37]$$

is the removal rate of component k in section l . For the often used first-order removal rate, i.e., $R = \bar{R}(v, t) n(v, t)$, [37] can be expressed as

$$\int_{v_{l-1}}^{v_l} \bar{v}_k \bar{R}(v, t) n(v, t) dv. \quad [38]$$

E. Multicomponent Sectional Equations

Combining the expressions in Eqs. [18], [20], [28], [29], [30], [36], and [37] we have for $l = 1, \dots, m$ and $k = 1, \dots, s$,

$$\begin{aligned} \frac{dQ_{l,k}}{dt} = & \frac{1}{2} \sum_{i=1}^{l-1} \sum_{j=1}^{l-1} \int_{v_{i-1}}^{v_i} \int_{v_{j-1}}^{v_j} \theta(v_{l-1} < u + v < v_l) (\bar{u}_k + \bar{v}_k) \beta(u, v) n(u, t) n(v, t) du dv \\ & - \sum_{i=1}^{l-1} \int_{v_{i-1}}^{v_i} \int_{v_{l-1}}^{v_l} \theta(u + v > v_l) \bar{u}_k \beta(u, v) n(u, t) n(v, t) du dv \\ & + \sum_{i=1}^{l-1} \int_{v_{i-1}}^{v_i} \int_{v_{l-1}}^{v_l} \theta(u + v < v_l) \bar{v}_k \beta(u, v) n(u, t) n(v, t) du dv \end{aligned}$$

$$\begin{aligned}
& - \frac{1}{2} \int_{v_{l-1}}^{v_l} \int_{v_{l-1}}^{v_l} \theta(u + v > v_l) (\bar{u}_k + \bar{v}_k) \beta(u, v) n(u, t) n(v, t) du dv \\
& - \sum_{i=l+1}^m \int_{v_{i-1}}^{v_i} \int_{v_{l-1}}^{v_l} \bar{u}_k \beta(u, v) n(u, t) n(v, t) du dv \\
& + \int_{v_{l-1}}^{v_l} \left\{ \int_0^1 \cdots \int_0^1 F_k(\eta_1 v, \dots, \eta_s v) P d\eta_1 \cdots d\eta_{s-1} \right\} n(v, t) dv \\
& + \int_{v_{l-1}}^{v_l - v'_k} v'_k \left\{ \int_0^1 \cdots \int_0^1 G_k(\eta_1 v, \dots, \eta_s v) P d\eta_1 \cdots d\eta_{s-1} \right\} n(v, t) dv \\
& - \sum_{i=1}^s \int_{v_{l-1} - v'_i}^{v_l} v \left\{ \int_0^1 \cdots \int_0^1 \eta_k G_i(\eta_1 v, \dots, \eta_s v) P d\eta_1 \cdots d\eta_{s-1} \right\} n(v, t) dv \\
& + \sum_{i=1}^s \int_{v_{l-1} - v'_i}^{v_{l-1}} \left\{ \int_0^1 \cdots \int_0^1 (\eta_k v + \delta_{i,k} v'_i) G_i(\eta_1 v, \dots, \eta_s v) P d\eta_1 \cdots d\eta_{s-1} \right\} n(v, t) dv \\
& + \int_{v_{l-1}}^{v_l} \bar{v}_k S(v, t) dv - \int_{v_{l-1}}^{v_l} \bar{v}_k R[n(v, t), v, t] dv. \quad [39]
\end{aligned}$$

Note that the first, second, third, and ninth terms on the right-hand side of Eq. [39] are evaluated only for $l > 1$ and the fifth term is evaluated only for $l < m$.

Thus far no mathematical approximations have been required to obtain Eq. [39]. However, this set of equations is unclosed since $g_k(v, \eta_k)$ and $n(v, t)$ are not related to $Q_{l,k}$. Therefore, one must introduce at least two approximations to close the system.

To eliminate $n(v, t)$ it is convenient to approximate the size distribution as being constant within each section. With this approximation it can be shown (15) that the sectional equations will reduce to the exact integrodifferential equation for one-component aerosols as the number of sections is increased for a fixed particle size domain. Although this is the lowest order and thus the first of an infinite set of possible approximations, using a constant has the advantage that the size distribution, which is a time-dependent quantity, generally need not be repeatedly integrated over particle size as one integrates in time. Furthermore, in comparing the sectional solution to a higher-order method for a one-component

aerosol, excellent agreement was obtained with as few as 10 sections.

Therefore, for the first approximation the distribution of a conveniently chosen size variable will be taken as constant within each section. Although up to this point particle mass has been taken to be the size variable of interest, one often would like to express the distribution on a size basis other than particle mass, for example, particle diameter. Since there is only an integral constraint on the size distribution, i.e.,

$$Q_l(t) = \int_{v_{l-1}}^{v_l} v n(v, t) dv, \quad [40]$$

one can arbitrarily choose a size variable other than particle mass for which the distribution is constant within a section. Assuming that the size variable of interest is x , and is uniquely related to v by $x = f(v)$, we can define $\bar{q}_l(t)$, a constant within each section, by

$$v n(v, t) = \bar{q}_l(t) f'(v), \quad [41]$$

where $f'(v) = df/dv$. Substituting Eq. [41] into Eq. [40] we have

$$Q_l(t) = \bar{q}_l(t)[f(v_l) - f(v_{l-1})]. \quad [42]$$

Therefore, a plot of $\bar{q}_l(t)$ versus x will result in a series of step functions such that the area under each step is equal to $Q_l(t)$ and

$$n(v, t) = \frac{Q_l f'(v)}{v(x_l - x_{l-1})}, \quad [43]$$

where $x_l = f(v_l)$.

To eliminate $g_k(v, \eta_k)$ it is convenient to approximate the mean mass fractions of all particles within a section as being equal and thus independent of particle size within a section. Note that this approximation does not make any assumptions or restrictions on how composition is distributed for a given particle size. Also, note that as the section size decreases to the point that only a single particle size is contained within each section, the mean mass fraction of different particle sizes within a section must be equal since there is only one particle size in the section. Therefore, in the limiting case of a single particle size in each section the first two sectional approximations become exact. Thus for $v_{l-1} < v < v_l$ and $k = 1, \dots, s$,

$$\int_0^1 \eta_k g_k(v, \eta_k) d\eta_k \quad [44]$$

is independent of v within section l . By definition

$$\begin{aligned} \frac{vQ_{l,k}}{Q_l} &= \frac{v \int_{v_{l-1}}^{v_l} \int_0^1 v \eta_k g_k(v, \eta_k) n(v, t) d\eta_k dv}{\int_{v_{l-1}}^{v_l} v n(v, t) dv}. \quad [45] \end{aligned}$$

Using the second approximation the double integral in Eq. [45] can be separated to give

$$\frac{vQ_{l,k}}{Q_l} = v \int_0^1 \eta_k g_k(v, \eta_k) d\eta_k. \quad [46]$$

Using the definition of \bar{v}_k given in Eq. [9] we have that in section l

$$\bar{v}_k = \frac{vQ_{l,k}}{Q_l}. \quad [47]$$

Since all the coagulation and removal terms of Eq. [39] (i.e., terms 1–5 and 11 on the right-hand side), which contain $g_k(v, \eta_k)$, are given in terms of \bar{v}_k , they can be directly related to $Q_{l,k}$ ($l = 1, \dots, m$ and $k = 1, \dots, s$) by Eq. [47] without solving for $g_k(v, \eta_k)$. Note that the source term (i.e., the 10th term on the right-hand side of Eq. [39]) is independent of $n(v, t)$ and $g_k(v, \eta_k)$ and thus does not have to be related to $Q_{l,k}$. If F_k and G_k are linear functions, then

$$\begin{aligned} \int_0^1 \cdots \int_0^1 F_k(\eta_1 v, \dots, \eta_s v) P d\eta_1 \cdots d\eta_{s-1} \\ = F_k(\bar{v}_1, \dots, \bar{v}_s) \quad [48] \end{aligned}$$

and

$$\begin{aligned} \int_0^1 \cdots \int_0^1 G_k(\eta_1 v, \dots, \eta_s v) P d\eta_1 \cdots d\eta_{s-1} \\ = G_k(\bar{v}_1, \dots, \bar{v}_s) \quad [49] \end{aligned}$$

as shown by Eqs. [23] and [32], respectively. Hence, the sixth and seventh terms on the right-hand side of Eq. [39] can be replaced by Eqs. [23] and [32], respectively. If G_i is independent of particle composition, [33] and [34] (with all γ 's equal to zero except $\gamma_{0,i}$) can be used to express the eighth and ninth terms, respectively, on the right-hand side of Eq. [39], which would close Eq. [39].

For those cases in which P is unknown and the conditions needed to eliminate it from the intraparticle chemical reaction and gas-to-particle conversion terms are not valid, one may have to resort to using Eqs. [48] and [49] as a third approximation, regardless of the functional forms of F_k and G_k . Finally, as the fourth approximation, the expected value of $\eta_k G_i$ may have to be approximated by the product of the expected values of η_k and G_i to determine the mass flux crossing section boundaries by gas-to-particle conversion. It is important to note that the errors introduced by using

TABLE I
Sectional Coefficients for Eq. [50]

Symbol	Remarks	Coefficient ^a
1. Coagulation		
$^{1a}\bar{\beta}_{i,j,l}$	$^{1a}\bar{\beta}_{i,j,l} \neq ^{1a}\bar{\beta}_{j,i,l}$ $^{1a}\bar{\beta}_{i,j,l} = ^{1b}\bar{\beta}_{j,i,l}$ $1 < l \leq m$ $1 \leq i < l$ $1 \leq j < l$	$\int_{x_{l-1}}^{x_i} \int_{x_{j-1}}^{x_j} \frac{\theta(v_{l-1} < u + v < v_l) u \beta(u, v)}{uv(x_i - x_{l-1})(x_j - x_{j-1})} dy dx$
$^{1b}\bar{\beta}_{i,j,l}$	$^{1b}\bar{\beta}_{i,j,l} \neq ^{1b}\bar{\beta}_{j,i,l}$ $^{1b}\bar{\beta}_{i,j,l} = ^{1a}\bar{\beta}_{j,i,l}$ $1 < l \leq m$ $1 \leq i < l$ $1 \leq j < l$	$\int_{x_{l-1}}^{x_i} \int_{x_{j-1}}^{x_j} \frac{\theta(v_{l-1} < u + v < v_l) v \beta(u, v)}{uv(x_i - x_{l-1})(x_j - x_{j-1})} dy dx$
$^{2a}\bar{\beta}_{i,l}$	$^{2a}\bar{\beta}_{i,l} \neq ^{2a}\bar{\beta}_{l,i}$ $1 < l \leq m$ $1 \leq i < l$	$\int_{x_{l-1}}^{x_i} \int_{x_{l-1}}^{x_l} \frac{\theta(u + v > v_l) u \beta(u, v)}{uv(x_i - x_{l-1})(x_l - x_{l-1})} dy dx$
$^{2b}\bar{\beta}_{i,l}$	$^{2b}\bar{\beta}_{i,l} \neq ^{2b}\bar{\beta}_{l,i}$ $1 < l \leq m$ $1 \leq i < l$	$\int_{x_{l-1}}^{x_i} \int_{x_{l-1}}^{x_l} \frac{\theta(u + v < v_l) v \beta(u, v)}{uv(x_i - x_{l-1})(x_l - x_{l-1})} dy dx$
$^3\bar{\beta}_{l,l}$	$1 \leq l \leq m$	$\int_{x_{l-1}}^{x_l} \int_{x_{l-1}}^{x_l} \frac{\theta(u + v > v_l) (u + v) \beta(u, v)}{uv(x_l - x_{l-1})^2} dy dx$
$^4\bar{\beta}_{i,l}$	$^4\bar{\beta}_{i,l} \neq ^4\bar{\beta}_{l,i}$ $1 \leq l < m$ $i < i \leq m$	$\int_{x_{l-1}}^{x_i} \int_{x_{l-1}}^{x_l} \frac{u \beta(u, v)}{uv(x_i - x_{l-1})(x_l - x_{l-1})} dy dx$
2. Gas-to-particle conversion		
$^1\tilde{G}_{l,k}$	$1 \leq l \leq m$	$\int_{x_{l-1}}^{f(v_l - v_k')} \frac{v_k' G_k(\bar{v}_1, \dots, \bar{v}_s)}{v(x_l - x_{l-1})} dx$
$^2\tilde{G}_{l,i}$	$1 \leq l \leq m$	$\int_{f(v_l - v_l')}^{x_l} \frac{G_l(\bar{v}_1, \dots, \bar{v}_s)}{(x_l - x_{l-1})} dx$
$^3\tilde{G}_{l,k}$	$1 \leq l \leq m$	$\int_{f(v_l - v_k')}^{x_l} \frac{v_k' G_k(\bar{v}_1, \dots, \bar{v}_s)}{v(x_l - x_{l-1})} dx$
3. Intraparticle chemical reaction		
$\bar{F}_{l,k}$	$1 \leq l \leq m$	$\int_{x_{l-1}}^{x_l} \frac{F_k(\bar{v}_1, \dots, \bar{v}_s)}{v(x_l - x_{l-1})} dx$
4. Sources and removal mechanisms		
$\bar{S}_{l,k}$	$1 \leq l \leq m$	$\int_{v_{l-1}}^{v_l} \bar{v}_k S(v, t) dv$
$\bar{R}_{l,k}$	$\left\{ \begin{array}{l} \text{arbitrary order} \\ 1 \leq l \leq m \end{array} \right.$	$\int_{v_{l-1}}^{v_l} \bar{v}_k R[n(v, t), v, t] dv$
	$\left\{ \begin{array}{l} \text{first order} \\ 1 \leq l \leq m \end{array} \right.$	$Q_{l,k} \int_{x_{l-1}}^{x_l} \frac{\bar{R}(v, t)}{(x_l - x_{l-1})} dx$

^a $x_i = f(v_i)$, $u = f^{-1}(y)$, $v = f^{-1}(x)$, $\bar{v}_i = vQ_{l,i}/Q_l$, $n(v, t) = Q_l f'(v)/[v(x_l - x_{l-1})]$.

the last two approximations do not vanish in the limiting case of a single particle size within each section. Also note that the same results as those obtained using the last two approximations can be obtained by assum-

ing that all particles within a section have identical compositions.

Using the sectional approximations, Eq. [39] can be reduced to the final form of the multicomponent sectional equations,

$$\begin{aligned} \frac{dQ_{l,k}}{dt} = & \frac{1}{2} \sum_{i=1}^{l-1} \sum_{j=1}^{l-1} [{}^1\bar{\beta}_{i,j,l} Q_{j,k} Q_i + {}^{1b}\bar{\beta}_{i,j,l} Q_{i,k} Q_j] - \sum_{i=1}^{l-1} [{}^{2a}\bar{\beta}_{i,l} Q_i Q_{l,k} - {}^{2b}\bar{\beta}_{i,l} Q_l Q_{i,k}] \\ & - \frac{1}{2} {}^3\bar{\beta}_{l,l} Q_l Q_{l,k} - Q_{l,k} \sum_{i=l+1}^m {}^4\bar{\beta}_{i,l} Q_i + \bar{F}_{l,k} Q_l + {}^1\bar{G}_{l,k} Q_l \\ & - \sum_{i=1}^s [{}^2\bar{G}_{l,i} Q_{l,k} - {}^2\bar{G}_{l-1,i} Q_{l-1,k}] + {}^3\bar{G}_{l-1,k} Q_{l-1} + \bar{S}_{l,k} - \bar{R}_{l,k}, \quad [50] \end{aligned}$$

where the $\bar{\beta}$'s, \bar{G} 's, \bar{F} , \bar{S} , and \bar{R} are given in Table I. Note that the 1st, 2nd, 3rd, 4th, 10th, and 11th terms on the right-hand side

of Eq. [50] are evaluated only for $l > 1$ and the 6th term is evaluated only for $l < m$. Since there are m sections and s com-

TABLE II

Sectional Coagulation Coefficients with Geometric Constraint ($v_{i+1} \geq 2v_i$, $i = 0, 1, 2, \dots, m-1$)

Symbol	Remarks	Coefficient ^a
${}^{1a}\bar{\beta}_{i,j,l} = {}^{1b}\bar{\beta}_{i,j,l}$	$i < l-1$ $j < l-1$	0
${}^{1a}\bar{\beta}_{i,l-1,l} = {}^{1b}\bar{\beta}_{l-1,i,l}$	$\begin{cases} 1 < l \leq m \\ i < l-1 \end{cases}$ $\begin{cases} 1 < l \leq m \\ i = l-1 \end{cases}$	$\begin{cases} \int_{x_{l-1}}^{x_l} \int_{f(v_{l-1}-v)}^{x_{l-1}} \frac{u\beta(u,v)}{uv(x_l - x_{l-1})(x_{l-1} - x_{l-2})} dydx \\ \int_{x_{l-1}}^{f(v_{l-1}-v_{l-1})} \int_{f(v_{l-1}-v)}^{x_{l-1}} \frac{u\beta(u,v)}{uv(x_{l-1} - x_{l-2})^2} dydx \\ + \int_{x_{l-1}}^{x_l} \int_{f(v_{l-1}-v_{l-1})}^{x_{l-1}} \frac{u\beta(u,v)}{uv(x_{l-1} - x_{l-2})^2} dydx \end{cases}$
${}^{1b}\bar{\beta}_{i,l-1,l} = {}^{1a}\bar{\beta}_{l-1,i,l}$	$1 < l \leq m$ $i < l-1$	$\int_{x_{l-1}}^{x_l} \int_{f(v_{l-1}-v)}^{x_{l-1}} \frac{v\beta(u,v)}{uv(x_l - x_{l-1})(x_{l-1} - x_{l-2})} dydx$
${}^{2a}\bar{\beta}_{i,l} = {}^{1a}\bar{\beta}_{i,l,l+1}$	$1 < l \leq m$ $1 \leq i < l$	$\int_{x_{l-1}}^{x_l} \int_{f(v_l-v)}^{x_l} \frac{u\beta(u,v)}{uv(x_l - x_{l-1})(x_l - x_{l-1})} dydx$
${}^{2b}\bar{\beta}_{i,l}$	$1 < l \leq m$ $1 \leq i < l$	$\int_{x_{l-1}}^{x_l} \int_{x_{l-1}}^{f(v_l-v)} \frac{v\beta(u,v)}{uv(x_l - x_{l-1})(x_l - x_{l-1})} dydx$
${}^3\bar{\beta}_{i,l} = {}^{21a}\bar{\beta}_{i,l,l+1}$	$1 \leq l \leq m$	$\begin{cases} \int_{x_{l-1}}^{f(v_l-v_{l-1})} \int_{f(v_l-v)}^{x_l} \frac{(u+v)\beta(u,v)}{uv(x_l - x_{l-1})^2} dydx \\ + \int_{x_{l-1}}^{x_l} \int_{f(v_l-v_{l-1})}^{x_l} \frac{(u+v)\beta(u,v)}{uv(x_l - x_{l-1})^2} dydx \end{cases}$
${}^4\bar{\beta}_{i,l}$	$1 \leq l < m$ $l < i \leq m$	$\int_{x_{l-1}}^{x_l} \int_{x_{l-1}}^{x_l} \frac{u\beta(u,v)}{uv(x_l - x_{l-1})(x_l - x_{l-1})} dydx$

^a $x_i = f(v_i)$, $u = f^{-1}(y)$, $v = f^{-1}(x)$.

Note that the expressions given for ${}^3\bar{\beta}$ and ${}^4\bar{\beta}$ are valid even if the geometric constraint is not satisfied. However, if the geometric constraint is not satisfied, ${}^3\bar{\beta}_{i,l} > {}^{21a}\bar{\beta}_{i,l,l+1}$.

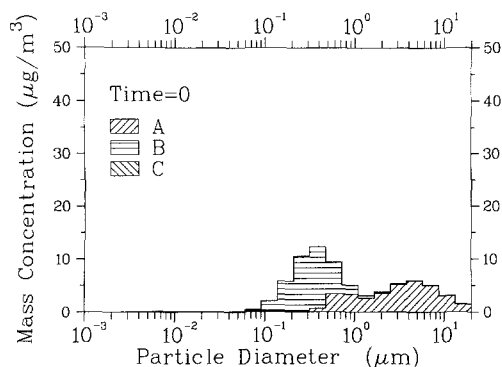


FIG. 1. Initial concentrations. Total mass concentration = $72.9 \mu\text{g m}^{-3}$.

ponents, Eq. [50] constitutes a set of $m \times s$ ordinary differential equations which are to be integrated in time.

For the special case of a one-component aerosol, $Q_{i,k} = Q_i$ for all i and Eq. [50] reduces to Eq. [19] given in (15) for a coagulating aerosol in which mass is conserved. Note that ${}^1a\bar{\beta} + {}^1b\bar{\beta}$ and ${}^2a\bar{\beta} - {}^2b\bar{\beta}$ are equal to ${}^1\bar{\beta}$ and ${}^2\bar{\beta}$, respectively, from that work.

III. APPLICATIONS

A. Comments on Section Size and Plotting

The sectional equations as given by Eq. [50] are such that the section size is arbitrary. However, since the particle size range of interest is usually quite large, one can impose a geometric constraint on the section boundaries (i.e., $v_i \geq 2v_{i-1}$, $i = 1$,

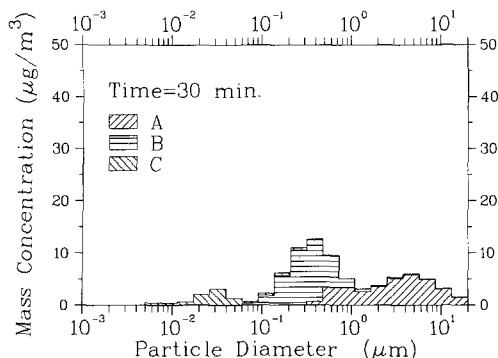


FIG. 2. Time evolution of multicomponent mass concentrations. Total mass concentration = $82.9 \mu\text{g m}^{-3}$.

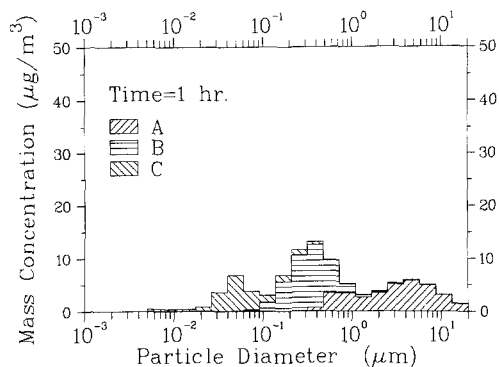


FIG. 3. Time evolution of multicomponent mass concentrations. Total mass concentration = $92.9 \mu\text{g m}^{-3}$.

\dots, m) without affecting most applications of the equations. With this constraint the minimum number of sectional coefficients is required since ${}^1a\bar{\beta}_{i,j,l} = {}^1b\bar{\beta}_{i,j,l} = 0$ for $i < l - 1$ and $j < l - 1$, ${}^2a\bar{\beta}_{i,l} = {}^1a\bar{\beta}_{i,l,l+1}$ and ${}^3\bar{\beta}_{i,l} = 2{}^1a\bar{\beta}_{i,l,l+1}$. Furthermore, by imposing the geometric constraint the sectional coagulation coefficients can be simply expressed without resorting to the use of a discontinuous θ function. Thus for some forms of $\beta(u, v)$ it may be possible to determine analytically the $\bar{\beta}$'s. The sectional coagulation coefficients for sections satisfying the geometric constraint are given in Table II. The reasoning by which one obtains Table II from Table I is given in (15).

In addition to selecting the section boundaries, one has considerable flexibility in choosing $f(v)$ and hence the type of plot to present the results of a simulation. For atmospheric aerosols one is usually interested in the shape of the distribution as represented versus $\log_{10}(D/1 \mu\text{m})$, where D is the particle diameter in micrometers. Thus, $f(v)$ for spherical particles will often be given as

$$f(v) = x = \log_{10} \left[\left(\frac{6v}{\pi\rho} \right)^{1/3} / 1 \mu\text{m} \right], \quad [51]$$

where ρ is the material density. A plot of the mass distribution $\bar{q}_i(t)$ versus x will then consist of a series of step functions where the contribution to each step in sec-

tion l due to component k is given by $\bar{q}_l(t)Q_{l,k}/Q_l$. One can also plot $Q_{l,k}$ versus x so that the mass of each component in each section can be determined directly. By adding the mass of all components in each section, the total aerosol mass in each section is given by the highest step in the section. Examples of such plots are given in Part III.B.

B. Coagulation of a Source-Reinforced Aerosol

The sectional equations were developed such that many complex and interacting processes can be simulated. However, to present a simple example for which the major features of the solution can be displayed, the evolution of a three-component source-reinforced coagulating aerosol will be simulated. Although virtually any initial size and chemical composition distribution can be used, for a representative example a trimodal size distribution which Whitby (16) has called "background and aged urban plume" was used. By assuming all particles initially consist of A, and rapid growth due to diffusion-controlled condensation of B produces larger particles, the mass fractions of A and B as a function of the new particle sizes can be determined from the initial and final particle sizes.² The mass of a component for a given particle size multiplied by the number distribution and integrated over each section

² Integrating the growth law given by Fuchs and Sutugin (17) for a set of initial particle sizes over a 1-sec interval determines the new set of particle sizes. The mass of B which is contained in the new particle sizes is found by subtracting the initial particle masses from the final particle masses. For the calculation $4D\Delta$ was chosen to be $1.0 \times 10^{-9} \text{ g cm}^{-1} \text{ sec}^{-1}$, where D is the diffusivity of the condensing species and Δ is the product of the molecular mass of B and the concentration difference of B above the particle surface and in the bulk phase. Since this calculation was done only to obtain a reasonable initial composition distribution, no correction factor (12) for particles approaching the size of the condensing molecules was used. A constant mean free path was also used in the calculations.

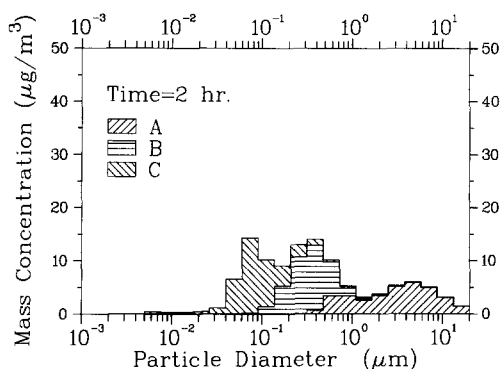


FIG. 4. Time evolution of multicomponent mass concentrations. Total mass concentration = $112.9 \mu\text{g m}^{-3}$.

provides the initial values of $Q_{l,k}$ as shown in Fig. 1 for A and B. Note that in Figs. 1–7, 20 logarithmically spaced sections over a range in particle diameter from 0.005 to $20.0 \mu\text{m}$ for $f(v)$ given by Eq. [51] were used. Therefore, the lower and upper bounds of section l are given by

$$0.005(4000)^{(l-1)/20} \mu\text{m} \quad [52]$$

and

$$0.005(4000)^{l/20} \mu\text{m}, \quad [53]$$

respectively. The material density was chosen to be 1.0 g cm^{-3} for all components. Fuchs' (18) coagulation coefficient (as given in (19)) was used at a temperature of 298°K and a mean free path of air of $0.066 \mu\text{m}$. To distinguish the source aerosol from the initial aerosol, the source consisted of pure C which was generated at $20 \mu\text{g m}^{-3} \text{ hr}^{-1}$ in the first section (i.e., in the particle diameter range from 0.005 to $0.00757 \mu\text{m}$), and no preexisting aerosol was placed in the first six sections (i.e., below a particle diameter of $0.0602 \mu\text{m}$).

Figures 1–7 show the evolution of $Q_{l,k}$ ($l = 1, \dots, 20$ and $k = 1, 2, 3$) for a 5-hr simulation. Notice in Figs. 1–3 that although C is being produced in the first section, it rapidly moves into the higher sections. Since there is no preexisting aerosol below a particle diameter of $0.0602 \mu\text{m}$, the movement of C must be due to the source particles coagulating among themselves and not the scavenging by preexist-

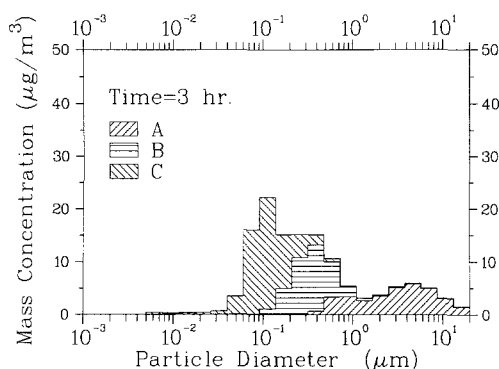


FIG. 5. Time evolution of multicomponent mass concentrations. Total mass concentration = $132.9 \mu\text{g m}^{-3}$.

ing aerosol. After 2 hr, Fig. 4 shows that the mode formed by the source is comparable to the mode primarily composed of B. However, Fig. 5 shows that after 3 hr the source particles have formed the dominant mode and the distribution has evolved from a trimodal to a bimodal distribution, for which the first peak occurs at about $0.1 \mu\text{m}$. As the source continually generates particles they are rapidly scavenged by existing aerosol. Since the scavenging of the source particles by the existing aerosol causes the existing particles to grow, the first peak in the mass distribution shifts to approximately $0.2 \mu\text{m}$ after 5 hr as shown in Fig. 7.

In comparing Figs. 1 and 7 we note that some mass of component B in the range 0.0911 to $0.209 \mu\text{m}$ has moved into the

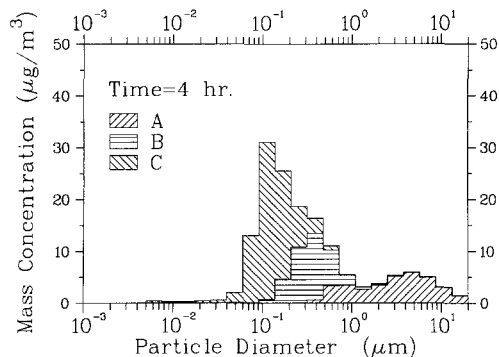


FIG. 6. Time evolution of multicomponent mass concentrations. Total mass concentration = $152.9 \mu\text{g m}^{-3}$.

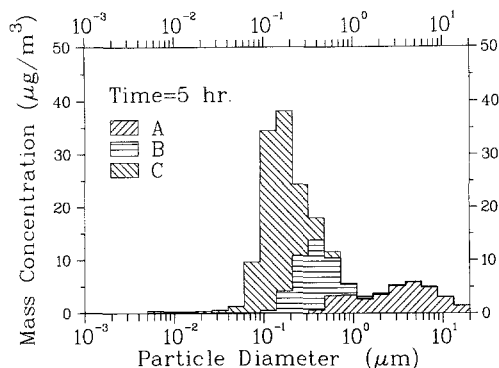


FIG. 7. Time evolution of multicomponent mass concentrations. Total mass concentration = $172.9 \mu\text{g m}^{-3}$.

range 0.316 to $0.725 \mu\text{m}$. Although a one-component sectional solution would provide the total mass in each section, one could not readily determine this movement and the relative masses of B and C in the range of 0.0911 to $0.725 \mu\text{m}$, which is clearly displayed in Fig. 7 using the multicomponent sectional equations.

Finally, we note that the calculations were performed up to a particle diameter of $20.0 \mu\text{m}$ to minimize the finite domain error (20), and contain nearly all of the modes reported by Whitby (16). However, because the number concentration above $1.10 \mu\text{m}$ is relatively small, hardly any changes in the mass distribution occurred above $1.10 \mu\text{m}$ even though a significant amount of aerosol mass is found in this region. Clearly, better resolution for essentially the same computational effort can be obtained by using the same number of sections but with an upper limit of $1.0 \mu\text{m}$.

IV. DISCUSSION

A. Computational Requirements

To obtain a solution one must determine the sectional coefficients and integrate a system of $m \times s$ ordinary differential equations. Since typically more than 50% of the computational effort is devoted to numerically evaluating the sectional coagulation coefficients, one should try to minimize the

number of these coefficients and store them for possible use in subsequent problems. Because the particle size range, section size, and coagulation mechanism of interest are usually the same for many atmospheric aerosol problems, one set of sectional coagulation coefficients can be used for problems with a different number of components, initial mass and composition distributions, and source, removal, growth, and reaction mechanisms.

The total number of sectional coagulation coefficients can be determined as follows. Using the fact that ${}^{1a}\bar{\beta}_{i,j,l} = {}^{1b}\bar{\beta}_{j,i,l}$, the number of coefficients for ${}^{1a}\bar{\beta}$ and ${}^{1b}\bar{\beta}$ for section $l \geq 2$ is $(l-1)^2$. Therefore, for m sections

$$\sum_{l=2}^m (l-1)^2 = \frac{2m^3 - 3m^2 + m}{6} \quad [54]$$

coefficients have to be determined. For ${}^{2a}\bar{\beta}$, ${}^{2b}\bar{\beta}$, and ${}^4\bar{\beta}$ there are $3m(m-1)/2$ coefficients and only m coefficients for ${}^3\bar{\beta}$. Thus, the maximum number of coefficients is

$$\frac{m^3 + 3m^2 - m}{3}. \quad [55]$$

However, if the geometric constraint is satisfied, ${}^{1a}\bar{\beta}_{i,j,l} = {}^{1b}\bar{\beta}_{i,j,l} = 0$ for $i < l-1$ and $j < l-1$, $2^{1a}\bar{\beta}_{l,l,l+1} = 2^{1b}\bar{\beta}_{l,l,l+1} = {}^3\bar{\beta}_{l,l}$, and ${}^{1a}\bar{\beta}_{i,l,l+1} = {}^{2a}\bar{\beta}_{i,l}$. Therefore, all ${}^{1a}\bar{\beta}$'s can be determined from the ${}^{2a}\bar{\beta}$'s and ${}^3\bar{\beta}$'s, and there are only

$$\sum_{l=3}^m l-2 = \frac{(m-2)(m-1)}{2} \quad [56]$$

nonzero independent coefficients for ${}^{1b}\bar{\beta}$. Since the number of coefficients for ${}^{2a}\bar{\beta}$, ${}^{2b}\bar{\beta}$, ${}^3\bar{\beta}$, and ${}^4\bar{\beta}$ is not affected by the geometric constraint, the total number of sectional coagulation coefficients reduces to its minimum value of $2m^2 - 2m + 1$.

B. Other Methods for Simulating Multicomponent Aerosol Dynamics

Although the sectional technique presented in this work is capable of simulat-

ing nearly all atmospheric multicomponent aerosol dynamics of interest, other possible alternatives should be considered. Therefore, for the remainder of this work, two other techniques as given in Table III will be discussed and compared to the multicomponent sectionalization method.

Because several techniques have been reported for computing size distribution dynamics of one-component systems (2, 5, 15, 20, 21), one approach to the multicomponent problem is to use a single variable such as the mass of one of the components in the particle to characterize the particle size and composition. Assuming that the characteristic component is conserved during coagulation, the masses of the nonconserved components in the particle may be determined by an auxiliary constraint, typically thermodynamic equilibrium. Such an approach has been reported for an $\text{H}_2\text{SO}_4\text{-H}_2\text{O}$ aerosol (12, 22, 23). In this case one may assume H_2SO_4 is the characteristic component that is conserved by coagulation, and the water content of the particle is determined by thermodynamic equilibrium. Therefore, only the distribution of H_2SO_4 with time is to be determined. Since this distribution can be represented by a curve fitted to m points, where m is typically 20 to 30, the solution to the m differential equations governing these points is required. Although an attractive feature of the approach is the small set of differential equations, one is greatly limited in the number of systems for which auxiliary constraints are valid and can be obtained. Therefore, the application of one-component aerosol equations is generally not well suited for multicomponent aerosol analysis.

Multicomponent sectionalization does not have these shortcomings, but requires s times as many equations, where s is the number of components in the aerosol. Average particle composition is determined as a function of particle size and time, and all components are con-

TABLE III
Methods for Simulating Multicomponent Aerosol Dynamics

Method	Number of differential equations ^a	Comments
One-component system	m	Thermodynamic equilibrium governs composition as a function of particle size. Coagulation is not conservative except for one component. Generally not well suited for multicomponent systems.
Multicomponent sectionalization	ms	Determines composition and concentration of particles as a function of particle size and time, but averages composition of particles of the same size. All processes are conservative.
s -Dimensional surface fitting	m^s	Determines concentration of particles of all sizes and compositions without any averaging. All processes are conservative.

^a m is the number of sections and s is the number of components.

served during coagulation, intraparticle chemical reaction, and gas-to-particle conversion. Because only the total mass of each component in a section is calculated, the relative concentration of particles of the same size with different compositions cannot be determined. For coagulation, sources and removal mechanisms, linear intraparticle reaction rates, and composition-independent gas-to-particle growth rates, the multicomponent sectional approximations become exact in the limiting case of a single particle size in each section. Therefore, for these processes virtually any degree of accuracy can be obtained for the total aerosol mass of each component as a function of particle size by increasing the number of sections for a fixed particle size domain. However, for nonlinear chemical reaction rates and particle-composition-dependent gas-to-particle growth rates, the sectional approximations introduce errors that do not vanish as the number of sections is increased. An analysis for the significance of these errors is beyond the scope of this work.

Finally, the third technique to consider as given in Table III is an s -dimensional surface fit of the multicomponent composition distribution function $\bar{n}(z_1, z_2, \dots, z_s)$, where z_i is the mass of component i in the particle and $\bar{n}(z_1, z_2, \dots, z_s)dz_1dz_2 \dots dz_s$

is the number of particles in the mass ranges $[z_1, z_1 + dz_1]$, $[z_2, z_2 + dz_2]$, \dots , $[z_s, z_s + dz_s]$ (14). Since \bar{n} is an s -dimensional surface, m^s equations are required to describe the evolution of the surface. Because no averaging is performed and all processes are conservative, as m increases a good approximate representation should reduce to the exact integrodifferential equation. Using this approach, one does obtain the relative concentration of particles of the same size with different compositions, and virtually any functional forms can be used for reaction and gas-to-particle conversion rates. However, the number of equations for realistic systems can be enormous. Even for the simple example given in Part III.B, the solution to 8000 equations would have been required, whereas only 60 equations were required for the multicomponent sectional technique. Therefore, although surface fitting would provide the most flexibility and detail of the methods discussed, the exponential increase in the number of differential equations with the number of components greatly limits application of this method.

V. CONCLUSION

Simulation of the dynamics of multicomponent aerosols has long been a com-

putationally intractable problem. The sectional approach developed in this work affords for the first time a feasible means of simulating multicomponent aerosol dynamics resulting from (i) coagulation, (ii) intraparticle chemical reaction, (iii) gas-to-particle conversion, and (iv) particle sources and removal mechanisms. This technique may now serve as a basis for the detailed modeling of atmospheric aerosols.

ACKNOWLEDGMENTS

This work was sponsored by the U. S. Nuclear Regulatory Commission in support of the advanced reactor safety research program at Sandia Laboratories. A portion of the work was supported by Environmental Protection Agency Grant R806844.

REFERENCES

1. Hidy, G. M., *J. Colloid Sci.* **20**, 123 (1965).
2. Berry, E. X., *J. Atmos. Sci.* **24**, 688 (1967).
3. Scott, W. T., *J. Atmos. Sci.* **25**, 54 (1968).
4. Drake, R. L., in "Topics in Current Aerosol Research" (G. M. Hidy and J. R. Brock, Eds.), Vol. 3, pp. 201-376. Pergamon, Oxford, 1972.
5. Suck, S. H., and Brock, J. R., *J. Aerosol Sci.* **10**, 581 (1979).
6. Brock, J. R., *Atmos. Environ.* **5**, 833 (1971).
7. Brock, J. R., *J. Colloid Interface Sci.* **39**, 32 (1972).
8. Gelbard, F., and Seinfeld, J. H., *J. Colloid Interface Sci.* **68**, 173 (1979).
9. Lindauer, G. C., and Castleman, A. W., *Aerosol Sci.* **2**, 85 (1971).
10. Burgmeir, J. W., Blifford, I. H., Gillette, D. A., *Water Air Soil Pollut.* **2**, 97 (1973).
11. Middleton, P., and Brock, J., *J. Colloid Interface Sci.* **54**, 249 (1976).
12. Gelbard, F., and Seinfeld, J. H., *J. Colloid Interface Sci.* **68**, 363 (1979).
13. Lushnikov, A. A., *J. Colloid Interface Sci.* **54**, 94 (1976).
14. Gelbard, F., and Seinfeld, J. H., *J. Colloid Interface Sci.* **63**, 472 (1978).
15. Gelbard, F., Tambour, Y., and Seinfeld, J. H., *J. Colloid Interface Sci.* **76**, 541 (1980).
16. Whitby, K. T., *Atmos. Environ.* **12**, 135 (1978).
17. Fuchs, N. A., and Sutugin, A. G., in "Topics in Current Aerosol Research" (G. M. Hidy, and J. R. Brock, Eds.), Vol. 2, pp. 34-35. Pergamon, Oxford, 1971.
18. Fuchs, N. A., "The Mechanics of Aerosols," pp. 291-294. Pergamon, New York, 1964.
19. Sitarski, M., and Seinfeld, J. H., *J. Colloid Interface Sci.* **61**, 261 (1977).
20. Gelbard, F., and Seinfeld, J. H., *J. Comput. Phys.* **28**, 357 (1978).
21. Turco, R. P., Hamill, P., Toon, O. B., Whitten, R. C., and Kiang, C. S., The NASA-Ames Research Center Stratospheric Aerosol Model I. Physical Processes and Computational Analogs, NASA Technical Paper 1362 (1979).
22. Hamill, P., *J. Aerosol Sci.* **6**, 475 (1975).
23. Hamill, P., Toon, O. B., and Kiang, C. S., *J. Atmos. Sci.* **34**, 1104 (1977).